Resilient Operation of Multiple Energy Carrier Microgrids

Saeed D. Manshadi, *Student Member, IEEE*, Mohammad E. Khodayar, *Member, IEEE*

Abstract — This paper proposed a methodology to identify the vulnerable components and ensure the resilient operation of coordinated electricity and natural gas infrastructures considering multiple disruptions within the microgrid. The microgrid demands which consist of electricity and heat demands are served by the interdependent electricity and natural gas supplies. The proposed approach addressed the vulnerability of multiple energy carrier microgrids against various interdictions, which is used to apply preventive reinforcements to increase the resilience of energy supply and decrease the operation cost. The proposed methodology is formulated as a bi-level optimization problem to address the optimal and secure operation of multiple energy carrier microgrids. The interdependence between natural gas and electricity infrastructures is addressed to show the effectiveness of the presented methodology in improving the resilience of generation and demand scheduling against deliberate actions causing disruptions in the interdependent energy infrastructures in multiple energy carrier microgrids.

Index Terms—multiple energy carrier microgrid, resilience, mixed integer bi-level linear programming, natural gas and electricity.

I. NOMENCLATURE

Variables

e	Index for electric energy
h	Index for heat energy
$f_{j,o}^{p}$	Natural gas flow in pipeline p between energy hubs j and o
$F_{\mathrm{c},i}$	Production cost function of thermal unit i
$F_{\mathrm{c},s}$	Natural gas supply volume cost at source s
i	Index for thermal generation unit
j,o	Energy hub indices
k	Index for heater unit
l	Index for distribution line
p	Index for natural gas pipeline
$P_j^{(.),d}$	Served demand in energy hub j
P_k^h	Heat energy produced by heater k
P_i^e, Q_i^e	Real/reactive generation dispatch of unit i
P_j^{inj}, Q_j^{inj}	Real/reactive power injection at energy hub j
$P_j^{i,d}$	Natural gas consumption of units i connected to energy hub j
$PL_{j,o}, QL_{j,o}$	Real/reactive power flow between energy hubs j and o
$\mathrm{Q}_j^{e,d}$	Served reactive electricity demand of energy hub j
s	Index for natural gas resource
UX_i	Availability status of generator unit i, 1 if interdicted, otherwise 0
$UY_{j,o}^{l}$	Availability status of transmission line l between energy hubs j and o, 1 if interdicted, otherwise 0
UZ_p	Availability status of natural gas pipeline p, 1 if interdicted, otherwise 0
V_j	Voltage magnitude at energy hub j
v_s	Natural gas supply volume of resource s
π_j	Natural gas pressure at energy hub j
θ_j	Voltage angle at energy hub j
λ, μ	Lagrangian multipliers

Constants

A	Energy hub-natural gas node incidence matrix
$B_{(.),(.)}$	Imaginary part of microgrid admittance matrix
$b_{j,o}$	Susceptance of the branch between energy hub j and o
C_p	Pipeline constant
$C_{(.)\_(.)}$	Coupling factors in energy conversion matrix
$f_{j,o}^{p,\max}$	Maximum flow for pipeline p between energy hubs j and o

The authors are with Electrical Engineering Department, Southern Methodist University, Dallas, TX. 75205 USA. (e-mails: manshadi@mail.smu.edu, and mkhodayar@lyle.smu.edu).

$G_{(.),(.)}$	Real part of microgrid admittance matrix
$g_{j,o}, y_{j,o}$	Conductance and admittance of the distribution line between energy hub j and o
GG_j	Set of units connected to energy hub j
HH_j	Set of heaters connected to energy hub j
GS_j	Set of natural gas resources connected to energy hub j
$L_{f,j}, L_{t,j}$	Set of distribution lines starting from /ending at energy hub j
$M_{(.)}$	Required resources for interdiction of each component type in microgrid
M	Total available resources for interdiction
NB	Number of energy hubs
NG	Number of electricity generation units
NL	Number of distribution lines
NP	Number of natural gas pipelines
$P_j^{(.),D}, Q_j^{e,D}$	Active/reactive electricity demand at energy hub j
$P_{f,j}$	Set of pipelines starting from energy hub j
$P_{t,j}$	Set of pipelines ending at energy hub j
$P_i^{\max}, \mathrm{Q}_i^{\max}$	Maximum real/reactive generation of unit i
$SL_{j,o}^{\max}$	Maximum capacity of distribution line between energy hubs j and o
$VOLL^{(.)}$	Value of lost load
$V^{\max}, V^{\min}$	Max/min voltage at each energy hub
$v_s^{\max}, v_s^{\min}$	Max/min natural gas supply volume of resource s
$\pi^{\max}, \pi^{\min}$	Max/min natural gas pressure at each energy hub
$\theta^{\max}, \theta^{\min}$	Max/min voltage angle at each energy hub
$x_{j,o}, r_{j,o}$	Line reactance and resistance between energy hubs j and o
π'_j	Initial natural gas pressure at energy hub j

II. Introduction

THE increase in penetration level of distributed energy resources (DERs) supplied by natural gas in electricity networks warrants the coordinated operation of electricity and natural gas distribution networks. The rising concerns over the reliability and quality of service in energy distribution networks promotes the concept of multiple energy carrier microgrids. Multiple energy carrier microgrid is referred to as an interconnected electricity and natural gas distribution network in which the electrical network is composed of a group of interconnected electrical demands and DERs that represent a single controllable entity within the electricity grid with the ability to operate in grid-connected and island modes. The natural gas distribution network within the microgrid is composed of several source points which are connected to the gas distribution network and a group of load points which represent electrical generation units or heat demands. Several literatures have addressed the interdependence of electricity and natural gas infrastructures in power systems. The model in [1] presents a fundamental understanding of the interdependent energy systems including coal, natural gas and electricity while ignoring the network constraints. The interdependence of natural gas and electricity infrastructures is discussed in [2], where the optimal operation of the interconnected natural gas-electricity network is affected by several factors including, physical characteristics of natural gas pipeline and electricity networks, operational procedures in electrical and natural gas distribution networks, types of electricity generating plants, availability of natural gas and electricity supply, transmission and delivery constraints in natural gas and electricity networks, and their respective volatile market prices. In [3], switching between fuel supplies in electricity generation is proposed as an effective approach to perform peak shaving on natural gas demand while enhancing the power system operation security. Several factors including the natural gas market price, natural gas pipeline pressure loss, and simultaneous demand peak in electricity and natural gas which causes price spikes in severe weather conditions and possible outages in natural gas pipelines; affect the power system operation by increasing congestions, price of electricity or even demand curtailment in severe conditions. A security-constrained short term generation scheduling in electrical networks is developed in [4]. The slow transient process in natural gas transmission networks was considered by a set of partial differential and algebraic equations in [5]. The proposed approaches addressed the effects of natural gas transmission network on power system security by implementing determined scenarios for possible contingencies in both energy infrastructures.

A framework for the comprehensive modeling of multiple energy delivery systems in which energy is converted within an energy hub is presented in [6]. Energy hub provides the features of input, output, storage, and conversion of multiple energy carriers. An integrated optimization framework which incorporates a simplified model for the network flow of the interdependent energy carriers is proposed in [7]. An approach for optimal scheduling of multiple energy networks including electricity, natural gas, and district heat is introduced in [8]. A linear formulation is proposed in [9] to solve the large-scale optimal energy flow in multiple energy delivery networks. An expansion planning framework within the electricity and natural gas distribution networks with high penetration of gas-fired distributed generation is presented in [10], which incorporates heuristic methodologies to find the optimal expansion planning strategies. Discussion in [11] expressed the savings gained by optimal operation of integrated electricity and natural gas networks. In [12], an integrated formulation of electricity and heat distribution networks to procure the optimal electricity and heat flow within a microgrid is presented.

This paper addressed the coupling between electricity and natural gas energy infrastructures within the microgrids which can affect the resilience of energy supply. The resilience of energy infrastructure is addressed by identifying vulnerable components in electricity and natural gas infrastructures. Deliberate interruptions do not occur frequently, but, when they do, they can be tragic. Quantitative probabilistic evaluation of such low-probability-high-consequence contingencies is very challenging, resource-demanding, and subjected to inaccuracies. Moreover, the outcome of a disruption strongly depends on the system operation conditions prior to the attack, as well as the available resources to the offenders, both of which are also highly uncertain. There are a number of publications addressed the contingencies as a consequence of threat in power systems [13]-[17]. Contingencies as a result of natural disasters, physical or cyber-attacks would extinguish the key elements of the electricity infrastructure and may lead to blackouts. The disruptions of energy supply in electric power grids caused by physical attacks are addressed in [14] which is presented as a bi-level mixed integer programming problem and solved by a heuristic approach. A model to protect the power network against a range of scenarios which lead to disruption in energy supply and blackouts is developed in [15]. The three-level attacker-defender-planner model presented in [16] as a multi-level mixed integer programming problem finds the optimal defense strategy in power system. Here, the interdependence between energy networks was pointed out as a potential improvement in finding the more realistic defense strategies. In [17], a tri-level optimization model is proposed for power network defense which is solved iteratively by forming nested bi-level optimization problem with budget constraints associated with defender and attacker assuming that the defended components are infallible once they are hardened. The physical disruption, modeled as a mixed-integer bi-level programming (MIBLP) problem in [18] ignores the interdependence of electricity and natural gas infrastructures. Here, the power system under attack is represented by dc power flow approximation, without offering any preventive guidelines for reinforcing the system.

Other publications emphasized the importance of considering the interdependencies between natural gas and electricity to improve resilience and reliability measures without quantifying the outcomes [19]-[20]. Since microgrids are developed to provide higher power quality and reliability for consumers, the resilience of energy supply is an important concern within microgrids. In this paper, the energy resource interdependence in microgrids is represented by implementing energy hubs, and preventive reinforcement strategies are offered to the microgrid operators following the resiliency analysis. The contributions of this paper are as follows:

- Modeling the disruption as a consequence of deliberate actions in multiple energy carrier microgrids considering the interdependence of natural gas and electricity infrastructures
- Identify the critical and vulnerable components in multiple energy carrier microgrids
- Quantify the consequences of disruption by calculating the operation cost of multiple energy carrier microgrid in contingencies
- Apply preventive reinforcement strategies to ensure the resilient operation of microgrids and determine the reinforcement outcomes

The results can be used by microgrid planners and operators to identify critical components whose reinforcement will improve the reliability and security measures within the microgrids. The paper is organized as follows: Section III introduces the basic components of the energy hub. Section IV describes the preventive reinforcement in cyber infrastructure to improve the resilience in the energy supply. Section V describes the problem formulation. Section VI presents a case study, to show the effectiveness of the proposed preventive reinforcement procedure, and section VII presents the conclusion.

III. Energy Hub

Energy infrastructure provides various services to industrial, commercial, and residential consumers. The optimal expansion planning and operation of various energy carriers are determined as a set of independent problems without taking the interdependencies and interactions of the energy carrier networks into account. Here, the nodes in the distribution network with energy conversion facilities are referred to as "energy hubs". The energy hub incorporates the interdependencies between natural gas, electricity and heat and provides operational flexibility within active distribution networks as shown in Figure 1.

Here, the heat energy is produced as a bi-product of electricity generation using natural gas in combined heat and power (CHP) units and curtailing the electricity demand at each hub would result in curtailment of heat demand, as the electricity drives the pumps to facilitate heat transfer in the energy hubs.

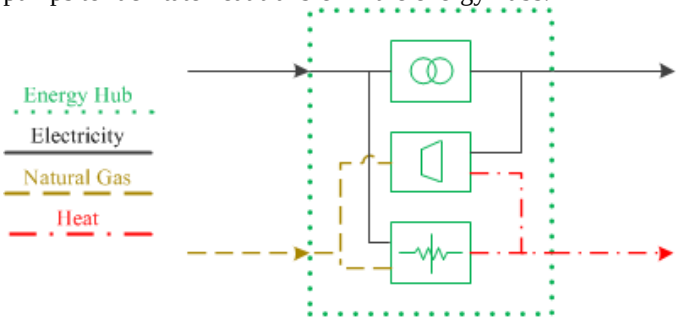

Fig.1. Energy hub with electricity, natural gas and heat

The interdependence of electricity and heat demands with electricity and natural gas resources provided at each energy hub is shown in (1), where the electricity and natural gas comprise input vector $\bar{\mathbf{E}}$, and the electricity and heat demand comprise output vector $\bar{\mathbf{L}}$. Here, matrix $\mathbf{C}$ is the forward coupling matrix which represents the input-output energy conversion. The forward coupling matrix is composed of coupling factors and is determined by characteristics and topology of the energy hub.

$$\underbrace{\begin{pmatrix} L_e \\ L_h \end{pmatrix}}_{\bar{\mathbf{L}}} = \underbrace{\begin{pmatrix} C_{e-e} & C_{gas-e} \\ C_{e-h} & C_{gas-h} \end{pmatrix}}_{\mathbf{C}} \underbrace{\begin{pmatrix} E_e \\ E_{gas} \end{pmatrix}}_{\bar{\mathbf{E}}} \tag{1}$$

IV. Preventive Reinforcement In Cyber Infrastructure

Multiple energy carrier microgrids ensure the continuity of service to critical demands in energy infrastructure. Hence the resilience of multiple energy carrier microgrids against cyber threats leading to disruptions in physical components in energy infrastructure is addressed. Multiple energy carrier microgrids cannot tolerate excessive restoration times, as the recovery and restoration is not considered as a viable option for the mission critical facilities served by microgrids. Hence the resilience is defined as the ability of the system to survive attacks without suffering from any service interruptions and the objective is to provide a solution framework to ensure the continuity of service in multiple energy carrier microgrids. The set of preventive actions that is required for resilient operation of microgrid, is defined through the proposed reinforcement procedure.

More than half of the cyber threads are in energy sector [21]. The most frequent cyber threats are authentication, denial of service, and buffer overflow [22]. Here, it is assumed that the objective of the attacker is to increase the service interruption by disrupting the physical components through cyber-attacks. The physical components of the microgrid receive encrypted data packets which contain the control signals from the microgrid controller. Hence decryption and manipulating the encrypted data packets would result in the disruption of the physical components. Figure 2 illustrates disruption of electricity distribution line by decrypting the control signals sent from the microgrid controller. Here, the disruption occurs if the encrypted data is decrypted and manipulated by the attacker. Moreover, it is assumed that the data packets correspond to each component is encrypted with an existing encryption technique e.g. secured hash functions (SHA-x) [23], or advanced encryption standard (AES) [24]. However, other encryption techniques [25] could also be applied in the proposed formulation. The higher encryption strength is achieved by the increase in the encryption cost which eventually leads to higher disruption cost of the physical component. The cost of providing higher encryption strength is dependent on the hardware implementations such as processing modules and communication channels. In this paper, an encryption cost is assigned to specific encryption strength provided by practical encryption techniques. For instance, the encryption cost of using AES-256 to encrypt a data packet is more compared to the encryption cost of using AES-192 considering the same performance measures. While the encryption strategy to improve the encryption strength of the data packets associated with the physical components are discussed in this paper, the incorporated encryption technique is out of the scope of this paper. The presented model considers an initial encryption strength for the data packets corresponding to each physical component. The new encryption strategy is to improve the encryption strength for the certain components which are identified by the solution of the bi-level optimization problem employed. Hence, an improved encryption strategy decreases the vulnerability of microgrid against disruptions and increase the cost of decryption, data manipulation, and disruption of the physical components. In other words, each stage of the preventive reinforcement corresponds to the encryption strategy chosen in the microgrid. The encryption strategy taken, includes the improvements in the encryption strength of the selected physical components of the microgrid.

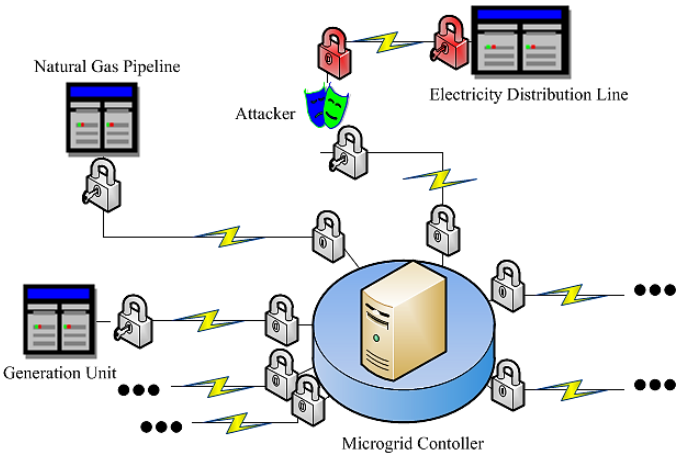

Fig.2. Disruption of service in multiple energy carrier microgrids

Here, it is assumed that different types of physical components in the microgrid require different numbers of data packets. The number of the data packets is dependent on the number of controllable variables in each component. For instance, it is assumed that generators require larger number of data packets for monitoring and control compared to the distribution lines.

The preventive reinforcement presented here is defined in several stages, where the microgrid resilience at each stage is dependent on the encryption strategy incorporated for monitoring and control of the microgrid. The solution to the bi-level optimization problem at each stage procures the new encryption strategy and the iterative procedure continues until the desired level of resilience is established. The desired level of resilience is determined by the microgrid planner or operator. To quantify the resilience of the microgrid against disruptions, a resilience index (r) shown in (2) is defined as the exponential of negative ratio of the increase in operation cost of multiple energy carrier microgrid as a result of disruptions to the budget of the attacker causing such disruptions. Here, γ and γ_0 are operation costs of disrupted and non-disrupted multiple energy carrier microgrid. Thus low resilience index indicates that the multiple energy carrier microgrid is highly vulnerable against disruptions.

$$r = \mathrm{e}^{-\left(\frac{(\gamma-\gamma_0)}{M}\right)} \tag{2}$$

V. Problem Formulation

The operation of multiple energy carrier microgrids exposed to disruptions is presented as a bi-level optimization problem. The upper level problem maximizes the operation cost of the system subjected to the limitation of resources to trigger disruptions while the lower level problem minimizes the operation cost of the multiple energy carrier microgrid under attack. Further, the MIBLP problem is re-formulated into a single-level mixed integer programming (MIP) problem employing the duality theory.

The objective function of the upper level problem, expressed by (3), maximizes the operation cost while the decision binary

variables are the outage statuses of generation units, natural gas pipelines, and power distribution lines. The operation cost of system includes the penalty cost for the load curtailments, hence maximizing the operation cost of the system by the attacker would lead to maximizing the curtailed demand and the generation cost in the microgrid. The resources for triggering outages in various components of microgrid are limited as indicated in (4). In bi-level optimization problem presented here, the lower level problem and its constraints are considered as constraints for the upper level problem [26]. The objective function of the lower level problem is the operation cost of the microgrid which includes the operation cost of generating electricity and heat energy from natural gas, as well as the penalty cost for electricity and heat demand curtailment as shown in (5). The real and reactive power injection is shown by (6) and (7), respectively. For the sake of simplicity the parameter C_{e-e} which represents the efficiency of the transformer is considered as unity. The real and reactive power limits for generation units are formulated in (8) and (9) respectively. The curtailed real and reactive demand at each energy hub is less than the total real and reactive demand as presented by (10) and (11) respectively. The admittance of each power line shown in (12) incorporates the binary variable representing the outage status of the component. The real/reactive power injection used for ac power flow is linearized in (13) and (14). Equations (15), (16) and (17) present the linearized formulation for real, reactive and apparent power transmitted through the distribution line. Here, ξ is an auxiliary parameter, which is dependent on the load power factor as calculated in [27]. The limitation on apparent power flow is imposed by distribution line capacity as given in (18). The limitations on voltage magnitude and voltage phase angle in electrical networks as well as the natural gas pressure within natural gas distribution network are presented in (19), (20) and (21), respectively. The minimum and maximum capacity for natural gas resources are shown in (22). The interdependence of electricity and heat demands is represented in (23), where *K* is a large number, which indicates that the heat distribution facility requires electricity to transfer the heat. Thus, electric demand curtailment at each energy hub would lead to heat demand curtailment. The heat demand is served by the electricity bi-product or burning natural gas in heater as shown in (24). The natural gas balance at each energy hub is presented by (25), in which the injected natural gas at each hub is equal to the withdrawn volume by the interconnected pipelines as well as the energy hub to serve the electricity and heat demand. The natural gas is converted into electricity and heat using the respective conversion factors. Here, any outage in natural gas supply will result in the outage of the supplied generator. The constraint on natural gas flow in distribution pipelines is given in (26). Here, the dependency of the natural gas flow on temperature which is discussed in [28] is ignored and the linear dependency of natural gas flow between two interconnected energy hubs and their pressures are expressed in (27).The served heat demand is lower than the total heat demand at each energy hub as shown in (28).

$$\max_{UX_i, UY^l_{j,o}, UZ_p} \gamma\left(UX_i, UY^l_{j,o}, UZ_p\right) \tag{3}$$

Subject to:

$$\sum_{i}^{NG} M_i \cdot UX_i + \sum_{l}^{NL} M_l \cdot UY^l + \sum_{p}^{NP} M_p \cdot UZ_p \le M \tag{4}$$

$$\gamma(UX_i, UY^l_{j,o}, UZ_p) = \min_{\substack{P_i^e, P_k^h, \\ P_j^{e,d}, P_j^{h,d}}} \begin{pmatrix} \sum_i \left(F_{c,i}(P_i^e)\right) + VOLL^e.(\sum_j P_j^{e,D} - P_j^{e,d}) \\ + \sum_k \left(F_{c,k}(P_k^h)\right) + VOLL^h.(\sum_j P_j^{h,D} - P_j^{h,d}) \end{pmatrix} \tag{5}$$

$$\sum_{i \in GG_j} P_i^e - \sum_{j \in D_j} P_j^{e,d} = P_j^{inj} \tag{6}$$

$$\sum_{i \in GG_j} Q_i^e - \sum_{j \in D_j} Q_j^{e,d} = Q_j^{inj} \tag{7}$$

$$P_i^{\min} \cdot (1 - UX_i) \le P_i^e \le P_i^{\max} \cdot (1 - UX_i) \tag{8}$$

$$Q_i^{\min} \cdot (1 - UX_i) \le Q_i^e \le Q_i^{\max} \cdot (1 - UX_i) \tag{9}$$

$$0 \le P_j^{e,D} - P_j^{e,d} \le P_j^{e,D} \tag{10}$$

$$0 \le Q_j^{e,D} - Q_j^{e,d} \le Q_j^{e,D} \tag{11}$$

$$y_{j,o} = g_{j,o} + Jb_{j,o} = \frac{r_{i,o} \cdot (1 - UY_{j,o})}{r_{j,o}^2 + x_{j,o}^2} - J \frac{x_{i,o} \cdot (1 - UY_{j,o})}{r_{j,o}^2 + x_{j,o}^2} \tag{12}$$

$$P_j^{inj} = \left(2V_j - 1\right) G_{j,j} + \sum_{o(o \ne j)}^{NB} \left(G_{j,o}\left(V_j + V_o - 1\right) + B_{j,o}\left(\theta_j - \theta_o\right)\right) \tag{13}$$

$$Q_j^{inj} = -\left(2V_j - 1\right) B_{j,j} + \sum_{o(o \ne j)}^{NB} \left(-B_{j,o}\left(V_j + V_o - 1\right) + G_{j,o}\left(\theta_j - \theta_o\right)\right) \tag{14}$$

$$PL_{j,o} = -G_{j,o}(V_j - V_o) + B_{j,o}(\theta_j - \theta_o) \tag{15}$$

$$QL_{j,o} = B_{j,o}(V_j - V_o) + G_{j,o}(\theta_j - \theta_o) \tag{16}$$

$$SL_{j,o} = PL_{j,o} + \xi_{j,o} QL_{j,o} \tag{17}$$

$$\left|SL_{j,o}\right| \le SL_{j,o}^{\max} \tag{18}$$

$$V^{\min} \le V_j \le V^{\max} \tag{19}$$

$$\theta^{\min} \le \theta_j \le \theta^{\max} \tag{20}$$

$$\pi^{\min} \le \pi_j \le \pi^{\max} \tag{21}$$

$$v_s^{\min} \le v_s \le v_s^{\max} \tag{22}$$

$$0 \le P_j^{h,d} \le K \cdot P_j^e \tag{23}$$

$$0 \le P_j^{h,d} \le \sum_{i \in GG_j} (C^i_{gas-h}) P_i^e / (C^i_{gas-e}) + \sum_{k \in HH_j} P_k^h \tag{24}$$

$$\sum_{s \in GS_j} A_j \cdot v_s - \sum_{p \in P_{f,j}} f_p + \sum_{p \in P_{t,j}} f_p = \sum_{k \in HH_j} \frac{P_k^h}{C^k_{(gas-h)}} + \sum_{i \in GG_j} \frac{P_i^e}{C^i_{(gas-e)}} \tag{25}$$

$$-f_{j,o}^{p,\max} \cdot (1 - UZ_p) \le f_{j,o}^p \le f_{j,o}^{p,\max} \cdot (1 - UZ_p) \tag{26}$$

$$f_{j,o}^p - K \cdot UZ_p \le \frac{C_p\left((\pi'_j \pi_j - \pi'_o \pi_o)\right)}{\sqrt{\left|\pi'^2_j - \pi'^2_o\right|}} \le f_{j,o}^p + K \cdot UZ_p \tag{27}$$

$$0 \le P_j^{h,d} \le P_j^{h,D} \tag{28}$$

The presented MIBLP problem formulation (3)-(28) is expressed in the general form by (29)-(34). By employing duality theory, the presented problem is transformed to single-level MIP problem presented by (35)-(42). The proposed bi-

level problem can be transformed to a single level MIP problem using KKT conditions or duality theory. Here, the duality theory is used to decrease the number of the binary-to-continuous variable multiplications, computation complexity and solving time [29]. The objective function (3) is represented by (29) and the disruption resource allocation constraint (4) is presented as (30), where ρ^* is the optimal solution of lower level problem (32). The binary variables in (31) are the decision vectors representing the outage statuses of electricity generation and distribution components as well as the natural gas pipelines. The lower minimization problem, with determined binary variables, given in (32) represents (5) which minimizes the operation cost of the microgrid. Equations (33) and (34) represent all the equality and inequality constraints shown in (6)-(28), respectively. Here λ and μ are introduced as the dual variables associated with equality constraints (33) and inequality constraints (34), respectively.

$$\max_{U} h(\mathrm{U}, \rho^*) \tag{29}$$

Subject to:

$$g(U, \rho^*) \geq 0 \tag{30}$$

$$U \in \{0,1\} \tag{31}$$

$$\min_{\rho} d^T \rho \tag{32}$$

Subject to:

$$A(U) + B\rho = b_1 \qquad \lambda \tag{33}$$

$$C(U) + D\rho \geq b_2 \qquad \mu \tag{34}$$

In the presented single level MIP formulation (35)-(42), the objective is to maximize the operation cost of the system by determining the disruption binary variables U, generation dispatch ρ, equality constraint dual variable λ, and inequality constraint variable μ. The constraints (36)-(37) are similar to (30)-(31) and ρ^* is replaced by ρ, which is the decision variable in the equivalent problem (35)-(42). In the original formulation (29)-(34), the binary decision variables which are determined in the upper level problem (29)-(31) are fixed for the lower level problem (32)-(34). However, in (38), the dual form of the lower level problem is shown. In (39), it is stated that dual variables of the inequality constraints of the lower level problem are nonnegative. The constraints (40) and (41) are the same as (33) and (34), respectively. Here, U is the decision variable in the equivalent single level problem. The equality constraint associated with strong duality is expressed in (42). Here (38) and (42) are composed of several of binary-to-continuous variables multiplications, which are further linearized.

$$\max_{U,\rho,\lambda,\mu} h(\mathrm{U}, \rho) \tag{35}$$

Subject to:

$$g(U, \rho) \geq 0 \tag{36}$$

$$U \in \{0,1\} \tag{37}$$

$$B^T \lambda + D^T \mu = d \tag{38}$$

$$\mu \geq 0 \tag{39}$$

$$A(U) + B\rho = b_1 \tag{40}$$

$$C(U) + D\rho \geq b_2 \tag{41}$$

$$d^T \rho = \lambda^T [b_1 - A(U)] + \mu^T [b_2 - C(U)] \tag{42}$$

To solve the current problem, all the nonlinear terms which are composed of binary-to-continuous variable multiplication are transformed into linear forms. Such nonlinearities exist in three categories: a) the ac power flow formulation, b) the natural gas flow formulation, and c) the dual form of lower problem in the equivalent single level MIP problem. In the ac power flow formulation, the binary decision variables for the distribution lines are embedded in the admittance matrix as shown in (12). Equations (13)-(16) contain 10 binary-primal continuous variables multiplication terms, e.g. voltage as primal continuous variable to binary variable associated with distribution line availability status in (13). The second category is the natural gas flow formulations, as shown by equations (26) and (27). The last category is the dual form of the lower level problem, which has binary-to-continuous variable multiplications in (42). The linearized form of the term (43) is shown in (44)-(46) in which the lower and upper bounds of the continuous variable are considered as zero, and a large number, K, respectively. Here, Φ and Ψ are nonnegative continuous variables.

$$\Phi = U\mu, \quad U \in \{0,1\} \tag{43}$$

$$\Phi = \mu - \Psi \tag{44}$$

$$0 \leq \Phi \leq K \cdot U \tag{45}$$

$$0 \leq \Psi \leq K \cdot (1-U) \tag{46}$$

The constraint (27) is the linear approximation of the original Weymouth equation (47) which represents the relationship between the natural gas flow with the pressure at the inlet and the outlet of a natural gas pipeline. Figure 3 shows the hyper plane represented by Weymouth equation, which is decomposed into several smaller hyper planes. The linearization using Taylor series is valid only if the difference in natural gas pressure between the inlet and outlet of the pipeline is assumed to be limited, i.e. there is not significant pressure drop in the pipeline. This is a reasonable assumption for the short pipelines used in microgrids. The limitation on the node pressure on the gas pipeline network shown in (21) guarantees the accuracy of the approximation. The energy hubs within microgrids operate within specific range of nodal natural gas pressure, e.g. between 55 and 56 bars. The Weymouth equation is linearized around the initial point procured by solving optimal energy flow within the microgrid considering no disruptions.

$$f_{j,o}^{p} = C_p \cdot \sqrt{\pi_j^{\,2} - \pi_o^{\,2}} \tag{47}$$

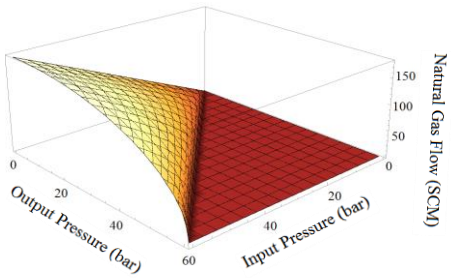

Fig.3. Hyper plane for the Weymouth equation

VI. Case Study

In this section, a multiple energy carrier microgrid composed of 10 energy hubs is illustrated in Figure 4. The microgrid presented in the case study operates in island mode; however, the presented preventive reinforcement procedure could be applied for microgrids operating in grid-connected mode by incorporating the grid interconnection with respective price of electricity and disruption cost into the formulation. The presented microgrid has 3 distributed generation CHP units with electrical and heat efficiency of respectively 34% and 50% which consume natural gas to produce electricity and heat, 11 electricity distribution lines, 10 electricity demands, 6 heat demands and 5 natural gas pipelines. Table I presents the characteristics of the natural gas generators. Table II lists the electricity and heat demands and their respective value of lost loads which determine the priority of demands. Table III describes the characteristics of electricity distribution lines and the natural gas pipelines.

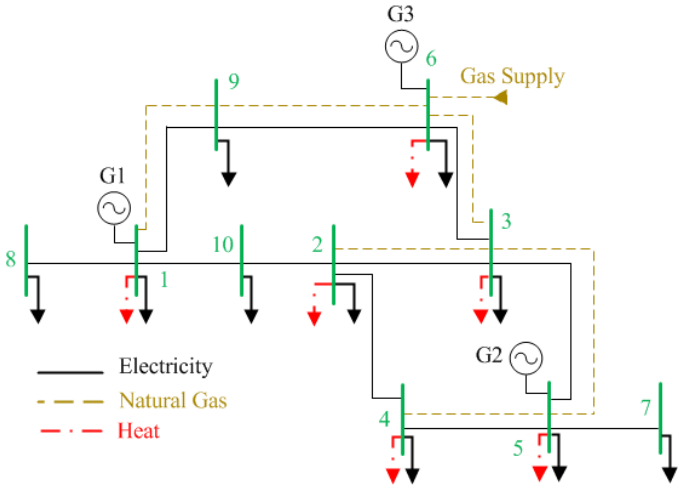

Fig. 4. Multiple energy carrier microgrid.

TABLE I
NATURAL GAS POWER GENERATION UNIT CHARACTERISTICS

Unit	P_{max}^1 (kW)	P_{max}^2 (kW)	F_c^1 (¢/kWh)	F_c^2 (¢/kWh)	$C_{gas-elec}^1$ (SCM/kWh)	$C_{gas-elec}^2$ (SCM/kWh)	P_{max} (kW)
G1	800	400	8	15	0.00789	0.0092	1,200
G2	1,200	600	10	28	0.00796	0.0102	1,800
G3	1,000	500	10	24	0.00726	0.0083	1,500

TABLE II
ELECTRICITY & HEAT DEMAND

Hub ID	$P^{e,D}$ (kW)	$Q^{e,D}$ (kVar)	$VOLL^e$ ($/kWh)	$P^{h,D}$ (MBtu)	$VOLL^h$ ($/MBtu)	π'_m (bar)
1	80.7	40.4	10	95.23	1	55.34
2	113.0	56.5	8	111.11	1	55.10
3	161.5	80.8	10	142.85	1	55.11
4	242.3	121.2	10	126.98	1	55.00
5	290.7	145.4	10	158.72	1	55.01
6	323.0	161.5	10	158.72	1	55.37
7	80.7	40.4	100	-	-	-
8	161.5	80.8	10	-	-	-
9	323.0	161.5	10	-	-	-
10	323.0	161.5	20	-	-	-

Here, C_p for natural gas pipeline is a constant which is determined by temperature, diameter, gas composition, length and friction [4]. The natural gas supply could deliver maximum volume of 50 Standard Cubic Meter (SCM) at the source point. The voltage magnitude and phase angles of energy hubs within the electrical distribution network are restricted between 0.95-1.05 per unit and $-\pi$ to π respectively. The resistance and inductive reactance of the distribution network cables are $r = 0.028\Omega/1000\,ft$ and $x = 0.037\Omega/1000\,ft$ respectively. The natural gas pressure at each hub is limited between 55 and 56 bars. The equivalent single level MIP is solved by IBM ILOG CPLEX v12.6.0 software package.

TABLE III
DISTRIBUTION NETWORK CHARACTERISTICS
(ELECTRICITY AND NATURAL GAS)

ID	From Hub	To Hub	Length (m)	SL^{max} (KVA)	C_p	f^{max} (SCM)
L1	1	8	100	1,200	-	-
L2	1	10	120	1,200	-	-
L3	1	9	160	2,000	-	-
L4	6	9	180	800	-	-
L5	10	2	120	1,000	-	-
L6	3	2	80	800	-	-
L7	6	3	140	1,700	-	-
L8	2	4	270	1,200	-	-
L9	3	5	350	1,200	-	-
L10	5	4	200	1,200	-	-
L11	5	7	300	1,000	-	-
P1	1	6	340	-	3	25
P2	2	3	80	-	2.82	25
P3	6	3	140	-	3	25
P4	3	5	350	-	2.82	25
P5	4	5	200	-	2.82	25

As stated earlier, an encryption cost is associated with a specific encryption strength provided by the practical encryption techniques. For example, the encryption costs of a single data packet using AES-128, AES-192, and AES-256 are assumed as $128, $256, and $512 respectively. Similarly, the encryption costs correspond to the hash function with 128, 256, and 512 bits could be assumed as $128, $256, and $512 respectively. Any Further improvement in encryption strength achieved by cascading encryption using the standard encryption techniques. The required resources to manipulate an encrypted data packet is assumed to be 10 times of the encryption cost. Here, the encryption and disruption costs of the initial encryption strength for each data packet are assumed as $128 and $1,280 respectively. The generator, natural gas pipeline, and electricity distribution line use 7, 6, and 2 data packets. Hence the disruption costs are $8,960, $7,680, and $2,560 for generator, natural gas pipeline and distribution line, respectively. Disruption attempts with limited resources ($20,000) were considered in the following cases to evaluate the resilience of the energy supply in the proposed microgrid:

- Case 1: No preventive reinforcement in the microgrid
- Case 2: First stage of preventive reinforcement, by increasing the disruption costs for the vulnerable components determined in Case 1.
- Case 3: Second stage of preventive reinforcement by increasing the disruption costs for the vulnerable components determined in Case 2.

- Case 4: Third stage of preventive reinforcement by increasing the disruption costs for the vulnerable components determined in Case 3.

A. Case 1: No preventive reinforcement in the microgrid

In this section, the impact of disruptions on the energy infrastructure within a microgrid is presented with no preventing reinforcement on the components. Applying the proposed methodology highlights the vulnerable components of the microgrid against disruption. The attack in this case results in disruption of distribution lines L2, L3, L4, and L7 and the natural gas pipeline P4. This will lead to the curtailment in electricity demands on energy hubs 2, 3, 4, 5, 7, 9, and 10 as well as curtailment in heat demands on energy hubs 2, 3, 4, and 5. The operation cost increases from $195 in normal operation to $26,275 in this case. The resilience index of multiple energy carrier microgrid in this case is 0.2715. In this case, the electricity and heat demands on energy hubs 1 and 6 are served by generation unit supplied by the natural gas. Since the electric demand on energy hub 9 is larger than that on energy hub 8, the impact of disruption on energy hub 9 is higher; hence interruption on L3 and L4 will lead to disruption of electricity supply on energy hub 9. On the natural gas distribution network, the natural gas pipeline from energy hub 3 to energy hub 5 is the primary candidate for interruption and this interruption will disrupt the operation of generator G2. Moreover, disconnecting electricity distribution lines L2 and L7 will result in forming four isolated electrical networks, i.e. {2, 3, 4, 5, 7, 10},{1,8}, {6}, and {9} within the microgrid. The supply and demand balance is reached by curtailing the electricity and heat demand as required. The total supplied electricity by G1 and G3 in this case is 559.4 kW which is equal to the served demand in the islands composed of energy hubs {1, 8} and {6}, respectively. In this case, disruption of P4 left G2 without the gas supply, and the generation dispatch of G2 is zero; hence, the island formed by energy hubs {2, 3, 4, 5, 7, 10} is left without any available electricity generation. As a result, the electricity demand is curtailed in this island.

B. Case 2: First Stage of Preventive Reinforcement

In this case, the encryption strategy is updated which indicates higher encryption strength for the data packets utilized to control and monitor the vulnerable components identified by the solution of the bi-level optimization problem in Case 1. The encryption cost for each vulnerable component is twice as that of the initial encryption strength. This is represented by increasing the encryption cost of each data packet to $256 for the disrupted components. For instance, the encryption cost of each data packet corresponds to L2 is increased from the initial cost of $128 to $256 so L2 is reinforced against disruptions in this case, by spending $512 for the improved encryption strength. In this case, the interruption in distribution lines L1, L2, L6, L9, L10 and L11 will lead to the interruption in electricity demand in energy hubs 2, 4, 7, 8, and 10 and the interruption in heat demand in energy hubs 2, 4 and 5. The operation cost will decrease by 20.2% from $26,275 in Case 1, to $21,860 in this case and the resilience index is 0.3385 in this case.

Here, as the disruption cost of line L7 was doubled, this line is not a good candidate for disruption; instead, interruption in L6 will result in the electric demand curtailment and consequently heat demand curtailment on energy hub 2. Moreover, as energy hubs 7 and 8 are fed radially by lines L11 and L1 respectively, interruption of these lines will lead to the electricity demand curtailment on energy hubs 7 and 8. Disruption in L11 will lead to the load curtailment on energy hub 7 with very high value of lost load (VOLL). Higher VOLL on energy hub 10 provokes the interruption of lines L2, L6 and L10 which feeds the demand on energy hubs 2, 4 and 10. As seen in the previous case, disruption in L9 isolates energy hub 5 from energy hubs {1, 9, 6, 3}. In this case, several isolated energy hubs including {8}, {1, 9, 6, 3}, {10, 2, 4}, {5} and {7} are formed.

C. Case 3: Second Stage of Preventive Reinforcement

Similar to Case 2, the encryption strategy is updated based on the solution to the bi-level optimization problem in Case 2. In this case, L1, L8, L10 and L11 were disrupted which led to the electricity demand curtailment in energy hubs 4, 7, and 8 and the heat demand curtailment in energy hub 4. The encryption strategy employed in the second stage of the preventive reinforcement reduced the operation cost by 71.1% from that of Case 2. The operation cost in this case is $12,777 and the resilience index is 0.5331. Here, the disruptions in electricity distribution lines L8 and L10 result in the electricity and consequently the heat load curtailment in energy hub 4. In this case, the energy hub 4 is a good candidate for the offender as L8 which feeds this energy hub has not been reinforced in the previous reinforcement stages and still is vulnerable to attacks; hence, it requires lower resources for interdiction compared to other reinforced distribution lines supplying energy hubs 2 and 3. The heat demand is curtailed on energy hub 4 as a result of disruption in the electricity supply and the interdependence of heat and electricity, as shown in (23). Similar to Case 2, interruptions in L1 and L11 will cause electricity demand curtailment in energy hubs 8 and 7 respectively.

D. Case 4: Third Stage of Preventive Reinforcement

In this case, the electricity demand on energy hubs 1, 8, 9, and 10 were curtailed as a result of interruption on L4, L5, and P1. The operation cost in this case is $12,770 which shows a slight decrease compared to that of Case 3. The resilience index of multiple energy carrier microgrid is 0.5333 in this case. Moreover, the energy hubs 1, 8, 9, and 10 in the microgrid were isolated as a result of the disruption in L4 and L5 and G1 is shut down as a result of disruption in the pipeline P1. This will curtail the electricity and heat demand on energy hub 1 because of disruption in both electricity and natural gas supplies. Although the curtailed demand in this case is larger compared to that in Case 3, the operation cost is very close to that of Case 3 because of the higher VOLL for electricity demand on energy hub 7 which is not interrupted in this case.

E. Preventive reinforcement procedure

Increasing the number of iteration to reinforce the disrupted components will result in more costly disruptions and less outages in the natural gas and electricity infrastructures. The preventive reinforcement procedure will prioritize the components for further reinforcements to reduce the operation cost of the microgrids as a result of reduction in curtailed electricity and heat demands. For instance, in the fourth stage of the reinforcement, the electricity distribution lines L9 and

L11 are reinforced. With this preventive reinforcement, the operation cost is reduced by 51.5% compared to that of Case 4 and reached to $8,424. In addition, the resilience index is increased to 0.6627. Table IV shows the operation cost, reinforcement cost, disrupted components and respective resilience index at each stage of reinforcement.

It is assumed that the encryption cost and consequently the disruption cost for the interrupted components will double at each stage as a result of the applied reinforcements. Figure 5 illustrates the reduction in the operation cost of the disrupted microgrid achieved by improving the encryption strategy at each stage of the preventive reinforcement. By comparing Case 1 with Case 4, it is observed that with the increase in disruption cost of the natural gas and electricity distribution network components, fewer islands are formed within the microgrid and the disruptions would be on the more expensive components which have not been reinforced earlier such as electricity generators in each island. It is also shown that the electricity and heat demands with higher VOLL are the primary targets for disruption, and consequently, the electricity distribution and natural gas pipelines supplying the energy hubs serving high priority demands are the first options for preventive reinforcements. By adding the operation cost and the reinforcement cost, the total cost at each stage of reinforcement is procured, which is shown in Figure 5. As shown in this figure, the minimum reinforcement and operation cost is achieved at sixth stage of reinforcement. At this stage, the total cost is $23,090. Hence, deploying the preventive reinforcement beyond this stage increases the investment cost on improving the encryption strategy beyond the increase in the operation cost as a result of disruption.

TABLE IV
OUTCOMES OF PREVENTIVE REINFORCEMENT PROCEDURE

Stage	Operation cost ($)	Resilience Index (r)	Disrupted Component	Total Encryption Cost ($)
0	26,275	0.2715	P4, L2, L3, L4, L7	9,344
1	21,860	0.3385	L1, L2, L6, L9, L10,L11	11,136
2	12,777	0.5331	L1,L8 L10,L11	12,298
3	12,770	0.5333	P1,L4,L5	14,720
4	8,424	0.6627	L9, L11	16,512
5	6,753	0.7205	G3, L3, L7	18,048
6	3,122	0.8639	L8, L10	19,968
7	1,924	0.9172	L1, P2	21,504
8	753	0.9725	P3	23,296
9	497	0.9851	P4	24,064
10	322	0.9937	P5	25,600
11	307	0.9945	P1	26,368
12	307	0.9945	P2	27,904
13	307	0.9945	P2	28,672
14	211	0.9993	G1	29,440
15	210	0.9993	G2	31,232
16	200	0.9998	G3	33,024
17	195	1	-	33,920

As shown in Table IV, after 17 stages of reinforcement, the microgrid is totally resilient to disruption attempts with limited resources ($20,000 in this case study). More resources for disruptions will result in more reinforcement steps within the multiple energy carrier microgrid. Figure 5 shows that as the reinforcement cost increases, the operation cost of the microgrid which reflects the lost electricity and heat demand, decreases.

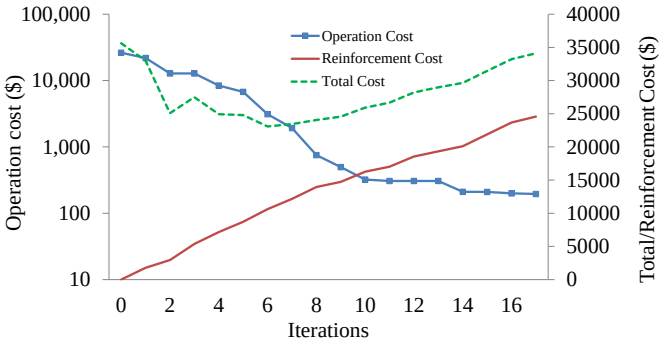

Fig. 5. Operation and reinforcement costs of multi-energy carrier microgrid.

VII. CONCLUSION

This paper introduced a methodology to analyze the resilience of microgrids with multiple energy carrier networks exposed to interruptions in electricity and natural gas distribution networks. The vulnerability of multiple energy carrier microgrids is addressed by introducing energy hubs which emphasizes the interdependence of electricity and natural gas energy infrastructures. It is shown that disruption in an energy network within the microgrid has adverse effects on other interdependent energy networks serving electricity and heat demands. It is observed that in order to maximize the adverse effects of disruptions the attacker inclines to create isolated networks within the microgrid as shown in Cases 1, 2, and 4. The proposed methodology suggests the reinforcement strategies for microgrid operators and investors by highlighting the vulnerable components and procuring the disruption outcomes as a result of component failures considering the interdependence of multiple energy infrastructures within the microgrid. The recommended preventive reinforcement warrants the resilient operation of multiple energy carrier microgrids considering limited reinforcement budget and the desired level of resilience. This paper is focused on proposing a methodology to identify the vulnerable components and ensure the resilient operation of coordinated electricity and natural gas infrastructures considering multiple disruptions within the microgrid. Although the diverse load scenarios with different values of lost load in multiple periods would result in a different preventive reinforcement plans for the operation period, the preventive reinforcement procedure remains the same. Defining the multi-period problem requires a detailed definition of the attacks addressing the length of interruption for each attack and the restoration time for the components if exists. This problem could be addressed as the future work for this paper.

VIII. REFERENCES

[1] A. Quelhas, E. Gil, J. McCalley, S. M. Ryan, "Multiperiod Generalized Network Flow Model of the U.S. Integrated Energy System: Part I—Model Description," *IEEE Trans. Power Syst.*, vol. 22, no. 2, pp. 829-836, May 2007.

[2] M. Shahidehpour, Y. Fu, and T. Wiedman, "Impact of natural gas infrastructure on electric power systems," *Proc. IEEE*, vol. 93, no. 5, pp. 1042–1056, May 2005.

[3] T. Li, M. Eremia, and M. Shahidehpour, "Interdependency of Natural Gas Network and Power System Security*," IEEE Trans. Power Syst.,* vol. 23, no. 4, pp. 1817-1824, Nov. 2008.

[4] C. Liu, M. Shahidehpour, Y. Fu, and Z. Li," Security-Constrained Unit Commitment Problem with Natural Gas Transmission Constraints," *IEEE Trans. On Power Syst.*, vol. 24, no. 3, pp. 1523-1536, Aug. 2009.

[5] C. Liu, M. Shahidehpour, and J. Wang, "Coordinated scheduling of electricity and natural gas infrastructures with a transient model for natural gas flow," *Chaos J.*, vol. 21, Jun. 2011.

[6] T. Krause, G. Andersson, K. Frohlich and A. Vaccaro, "Multiple-energy carriers: modeling of production, delivery, and consumption", *Proc. IEEE*, vol. 99, no. 1, pp.15 -27 2011.

[7] M. Geidl, and G. Andersson, "Optimal Power Flow of Multiple Energy Carriers," *IEEE Trans. On Power Syst.*, vol. 22, no. 1, pp. 145-155, Feb. 2007.

[8] M. Geidl and G. Andersson,"Operational and structural optimization of multi-carrier energy systems," *European Transactions on Electrical Power*, 16(5):463-477, 2006.

[9] M. Almassalkhi and I. Hiskens, "Optimization framework for the analysis of large-scale networks of energy hubs," *in Proc. 17th Power Syst .Computation Conf.*, Sweden, 2011.

[10] C. A. Saldarriaga, R. A. Hincapie, and H. Salazar, "A Holistic Approach for Planning Natural Gas and Electricity Distribution Networks," *IEEE Trans. Power Syst.*, vol. 28, no. 4, pp. 4052-4063, Nov. 2013.

[11] C. Unsihuay-Vila, J. Marangon-Lima, A. de Souza, I. Perez- Arriaga, and P. Balestrassi, "A model to long-term, multiarea, multistage, and integrated expansion planning of electricity and natural gas systems," *IEEE Trans. Power Syst.*, vol. 25, no. 2, pp. 1154–1168, May 2010.

[12] B. Awad, J. Wu, J. Ekanayake, and N. Jenkins, "Integrated optimal power flow for electric power and heat in a MicroGrid,"– Part1, 20th Intenational Conf. and Exhib. Elec. Dist, Czech Repubic, 2009.

[13] "Terrorism and the Electric Power Delivery System," Nat. Acad. Science, Nat. Res. Council study rep., 2012.

[14] J. Salmeron, K. Wood, and R. Baldick, "Analysis of electric grid security under terrorist threat," *IEEE Trans. Power Syst.*, vol. 19, no. 2, pp. 905–912, May 2004.

[15] D. Bienstock and S. Mattia, "Using mixed-integer programming to solve power grid blackout problems," *Discrete Optimization*, vol. 4, pp. 115–141, 2007.

[16] N. Romero, N. Xu, L. K. Nozick, I. Dobson, and D. Jones, "Investment planning for electric power systems under terrorist threat," *IEEE Trans. Power Syst.*, vol. 27, no. 1, pp. 108–116, Feb. 2012.

[17] Yiming Yao; Edmunds, T.; Papageorgiou, D.; Alvarez, R., "Trilevel Optimization in Power Network Defense," *Systems, Man, and Cybernetics, Part C: Applications and Reviews, IEEE Transactions on* , vol.37, no.4, pp.712,718, July 2007

[18] A. L. Motto, J.M. Arroyo, and F.D. Galiana, "A mixed-integer LP procedure for the analysis of electric grid security under disruptive threat", *IEEE Trans. Power Syst.*, vol. 20, no. 3, pp. 1357-1365, Aug 2005.

[19] R. Zimmerman and C. E. Restrepo, "Analyzing cascading effects within infrastructure sectors for consequence reduction," *in Technologies for Homeland Security, IEEE Conference On*, 2009, pp. 165-170.

[20] S. M. Rinaldi, "Modeling and Simulating Critical Infrastructures and Their Interdependencies," *in Proc. of the 37th Annual Hawaii International Conference on System Sciences* (HICSS'04), (Big Island, HI, USA), IEEE Computer Society Press, Jan. 2004.

[21] ICS-CERT incident response summary report. 2013. Industrial Control Systems Cyber Emergency Response Team (ICS-CERT). https://ics-cert.us-cert.gov/sites/default/files/ICS-CERT_Monitor_April-June2013.pdf

[22] ICS-CERT incident response summary report. 2014. Industrial Control Systems Cyber Emergency Response Team (ICS-CERT). https://ics-cert.us-cert.gov/sites/default/files/Monitors/ICS-CERT_Monitor_ Jan-April2014.pdf

[23] I. Mironov, "Hash functions: Theory, attacks, and applications," [Online], *Microsoft Research*, Silicon Valley Campus, Nov. 2005.

[24] J. Daemen and V. Rijmen, *The Design of Rijndael*. Springer-Verlag, 2002.

[25] D.E. Denning, *Cryptography and Data Security*. Addison-Wesley, 1982.

[26] J. Bard, Practical Bilevel Optimization: Algorithms and Applications. Norwell, MA: Kluwer, 1998.

[27] M. E. Khodayar, M. Barati, and M. Shahidehpour, "Integration of high reliability distribution system in microgrid operation," *IEEE Trans. Smart Grid*, vol. 3, no. 4, pp. 1997–2006, Dec. 2012.

[28] A. Martinez-Mares, and C. R. Fuerte-Esquivel, " A Unified Gas and Power Flow Analysis in Natural Gas and Electricity Coupled Networks," *IEEE Trans. Power Syst.*, vol. 27, no. 4, pp. 2156–2166, Nov. 2012.

[29] J M. Arroyo, "Bilevel programming applied to power system vulnerability analysis under multiple contingencies," *IET Gen. Trans. Dist.*, vol. 4, no. 2, pp. 178–190, Feb. 2010.

Saeed Dehghan Manshadi (S'14) received the B.S. degree in electrical engineering from the School of Electrical and Computer Engineering, University of Tehran, Tehran, Iran, in 2012, and the M.S. degree in electrical engineering from the State University of New York, Buffalo, NY, USA, in 2014. He is currently pursuing the Ph.D. degree in electrical engineering from the Department of Electrical Engineering, Southern Methodist University, Dallas, TX, USA. His current research interests include microgrids, bi-level optimization, and power system operation and planning.

Mohammad E. Khodayar (M'12) received his B.S. degree from Amirkabir University of Technology, Tehran, Iran; M.S. degree from Sharif University of Technology, Tehran; and Ph.D. degree from IIT, Chicago, IL, USA, in 2012, all in electrical engineering. He was a Senior Research Associate with the Robert W. Galvin Center for Electricity Innovation at IIT. He is currently an assistant professor with the Department of Electrical Engineering, Southern Methodist University, Dallas, TX, USA. His current research interests include power system operation and planning.